Heliyon 10 (2024) e30388

Contents lists available at ScienceDirect

Heliyon

journal homepage: www.cell.com/heliyon

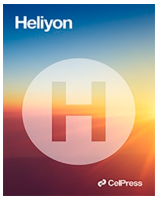

Research article

Mechanism of lncRNA SNHG16 on kidney clear cell carcinoma cells by targeting miR-506-3p/ETS1/RAS/ERK molecular axis

Tao Cheng, Ming-Li Gu *, Wei-Qiang Xu, Da-Wen Ye, Ze-Yu Zha, Wen-Ge Fang, Li-Kai Mao, Jing Ning, Xing-Bang Hu, Yong-Hui Ding

Department of Urology, The Second Affiliated Hospital of Bengbu Medical College, Bengbu, Anhui, 233000, China

A R T I C L E I N F O

Keywords:
lncRNA SNHG16
miR-506-3p
ETS1
RAS/ERK signaling pathway
Kidney clear cell carcinoma
Proliferation and migration

A B S T R A C T

Objective: This study aimed to investigate the mechanism of long noncoding ribonucleic acid (lncRNA) SNHG16 on kidney clear cell carcinoma (KIRC) cells by targeting miR-506-3p/ETS proto-oncogene 1, transcription factor (ETS1)/RAS/Extracellular regulated protein kinases (ERK) molecular axis, thus to provide reference for clinical diagnosis and treatment of KIRC in the future.

Methods: Thirty-six patients with KIRC were enrolled in this study, and their carcinoma tissues and adjacent tissues were obtained for the detection of SNHG16/miR-506-3p/ETS1/RAS/ERK expression. Then, over-expressed SNHG16 plasmid and silenced plasmid were transfected into KIRC cells to observe the changes of their biological behavior.

Results: SNHG16 and ETS1 were highly expressed while miR-506- 3p was low expressed in KIRC tissues; the RAS/ERK signaling pathway was significantly activated in KIRC tissues ($P < 0.05$). After SNHG16 silence, KIRC cells showed decreased proliferation, invasion and migration capabilities and increased apoptosis rate; correspondingly, increase in SNHG16 expression achieved opposite results ($P < 0.05$). Finally, in the rescue experiment, the effects of elevated SNHG16 on KIRC cells were reversed by simultaneous increase in miR-506-3p, and the effects of miR-506-3p were reversed by ETS1. Activation of the RAS/ERK pathway had the same effect as increase in ETS1, which further worsened the malignancy of KIRC. After miR-506-3p increase and ETS1 silence, the RAS/ERK signaling pathway was inhibited ($P < 0.05$). At last, the rescue experiment (co-transfection) confirmed that the effect of SNHG16 on KIRC cells is achieved via the miR-506-3p/ETS1/RAS/ERK molecular axis.

Conclusion: SNHG16 regulates the biological behavior of KIRC cells by targeting the miR-506-3p/ETS1/RAS/ERK molecular axis.

1. Introduction

Renal cell carcinoma (RCC) accounts for approximately 4 % of all malignancies [1]. According to statistics, there are more than 60,000 new cases of RCC and about 15,000 deaths due to RCC in the United States each year, which also correlates significantly with the insensitivity of RCC to radiotherapy/chemotherapy [2,3]. Metastasis is one of the important biological properties of RCC [4]. Prognostic survival rate for advanced RCC less than 10 % [5]. Kidney clear cell carcinoma (KIRC) is the most common subtype (accounting

* Corresponding author.
E-mail address: gumingli2020@sina.com (M.-L. Gu).

https://doi.org/10.1016/j.heliyon.2024.e30388
Received 8 January 2024; Received in revised form 24 April 2024; Accepted 25 April 2024
Available online 26 April 2024

for more than 80 % of all RCC) of RCC with the highest rate of local invasion and metastasis, posing a great threat to patients [1,6].

long noncoding ribonucleic acid (lncRNA) are a recent hot topic in oncology research [7]. LncRNA regulate gene expression at the chromatin, DNA, and at both transcriptional and post-transcriptional levels, and influence the occurrence and outcome of various diseases [8,9]. Small nuclear RNA host genes (SNHGs), as one of the classes mentioned above, with 22 family members (SNHG1 to SNHG22), all of which are abnormally expressed in various tumors [10–12]. SNHG16 is located on human chromosome 17q25.1 and is first identified as an oncogene in neuroblastoma [13]. In recent years, the role of SNHG16 in KIRC has been gradually concerned; it has been confirmed that SNHG16 can participate in the development of KIRC through CDKN1A, STARD9, and other pathways, and is expected to a new direction in the diagnosis and treatment of KIRC [14,15]. Second, mitogen-activated protein kinase (MAPK) is one of the most important transduction pathways in cell signal transduction network [16,17]. Ras/ERK is one of the most classical signaling pathways, which is critical in many tumor diseases, including KIRC [18–20]. Through prediction analysis using online database Taxgetscan, miR-506-3p binding site was observed in the 3′UTA region of mRNA of downstream transcription factor ETS-1, and ETS-1 is related to transduction of Ras/ERK signaling pathway [21,22]. Therefore, SNHG1 may be involved in the miR-506-3p/ETS1/RAS/ERK molecular axis.

Therefore, this study aims to further explore the mechanism of action and pathway of SNHG16 in KIRC, so as to provide reference for future clinical application of SNHG16 in KIRC.

2. Materials and methods

2.1. Patient data

Thirty-six patients with KIRC who underwent surgery in The Second Affiliated Hospital of Bengbu Medical College from December 2020 to March 2022 were enrolled as study subjects with 42 healthy physical examiners during the same period. After ethical approval of our hospital and the consent of the patients were obtained, the surgically resected carcinoma tissues, adjacent tissues, peripheral blood from KIRC patients and medical examiners were collected. Inclusion criteria: Patient diagnosed with space-occupying lesions of the kidney preoperatively by ultrasound, CT (plain or enhanced), MRI (plain or enhanced), or other measures, and confirmed as KIRC by postoperative pathological examination. Exclusion criteria: Patients with other benign/malignant tumors, immune deficiency, cardiovascular dysfunction, neurological disease or (and) organ dysfunction (excluding in kidney); patients in pregnancy/lactation period; patients with a history of preoperative surgery or antibiotic treatment.

2.2. Quantitative real time polymerase chain reaction (qRT-PCR)

TotalRNA was extracted from kidney tissues and serum with TRIzol (Thermo Fisher, USA) and assessed for purity and concentration with Nan-oDrop 2000 spectrophotometer (Thermo Fisher, USA). The reaction volume was 20 μL, and the reverse transcription conditions were 37 °C for 15 min and 85 °C for 5 min. The first-strand cDNA was then used as a template for mRNA amplification. The primer sequences were designed and constructed by Jiangsu Saisofei Biotechnology Co (Table 1). Using GAPDH and U6 as controls, the expression of SNHG16/miR-506-3p/ETS proto-oncogene 1, transcription factor (ETS1)/RAS/Extracellular regulated protein kinases (ERK) was calculated by $2^{-\triangle\triangle CT}$.

2.3. Immunohistochemistry

Kidney tissue sections were fixed with 4 % paraformaldehyde, embedded in paraffin, and stored at −4 °C for 24 h. Gradient ethanol dehydration was followed by the use of sodium citrate buffer (10 mM, pH 6.0), flooding of the sections, and boiling in an autoclave to repair the antigen. Endogenous peroxidase, specific proteins were blocked, ETS1, RAS and ERK primary antibodies (1:500) (Abcam, USA) were added and incubated overnight at 4 °C. The following day, biotinylated secondary antibody (1:1000) (Abcam, USA) was added dropwise and incubated at 37 °C for 40 min. DAB was added dropwise for color development and hematoxylin for restaining, and the slices were subsequently blocked and observed under a microscope.

2.4. Western blot

Total protein was extracted using the lysate, determined by the bicinchoninic acid (BCA) (Merck, USA) assay (quantitative method)

Table 1
Sequence of primers.

	Forward primer (3′-5′)	Reverse primer (3′-5′)
SNHG16	GCAGAATGCCATGGTTTCCC	GGACAGCTGGCAAGAGACTT
ETS1	CCACAGACTTTGAGGGAAGC	CTGCTCTCAGCACCTCACTT
RAS	GCGCTGACCTAGGAATGTTG	AGGAGTAGTACAGTTCATGAC
ERK	CCAAGTCAGACTCCAAAGCC	GGTCATAGTACTGCTCCAGG
β-actin	CTGAGAGGGAAATCGTGCGT	CCACAGGATTCCATACCCAAGA
miR-506-3p	GCCACCACCATCAGCCATAC	GCACATTACTCTACTCAGAAGGG
U6	CTCGCTTCGGCAGCACA	AACGCTTCACGAATTTGCGT

for concentration, added with an appropriate amount of loading buffer, and heated in boiling water for 10 min for protein denaturation to obtain the electrophoresis protein sample. The protein was transferred to Polyvinylidene Fluoride (PVDF) (Merck, USA) membrane by Sodium Dodecyl Sulfate PolyAcrylamide Gel Electrophoresis (SDS-PAGE) (Merck, USA) electrophoresis, blocked with skim milk powder at 37 °C for 2 h, washed with TPBS for 3 times, incubated with primary antibody (1:100) (Abcam, USA)overnight at 4 °C, then washed 3 times with TPBS and incubated with secondary antibody (1:50000) (Abcam, USA). A proper amount of developer (solution A:solution B = 1:1) was prepared and evenly smeared on the PVDF membrane, the target protein was scanned with the gel imaging system, and the gray value was analyzed with the software Image-Pro Plus using Glyceraldehyde-3-phosphate dehydrogenase (GAPDH) as the internal reference.

2.5. Cell data

Kidney carcinoma cell lines OSRC-2, ACHN, and 786-O were purchased from Shanghai Cell Bank of Chinese Academy of Sciences. They were cultured in RPMI 1640 medium containing 5 % fetal bovine serum, and cultured in normoxic conditions at 37 °C in an atmosphere containing 20 % O_2, 5 % CO_2, and 75 % N_2. Cells in logarithmic phase were obtained for the experiment. They were divided into blank group, mimics group and si-SNHG16 group.

2.6. Cell transfection

The cells were seeded in 6-well plates at 1×10^5 cells/mL, and transfected when the cells grew to 80 % according to the instruction for use of the Lipofectamine™ 2000 (Thermo Fisher, USA) Transfection Reagent. Different volumes of siRNA plasmid and transfection reagent were separately diluted with 250 μL of reduced serum medium; the blank group was transected with SNHG16, the mimics group with over-expressed SNHG16 plasmid, and the si-SNHG16 group with SNHG16 expression-interfered plasmid. The expression of SNHG16 was determined by qRT-PCR for the success rate of transfection, and the expression of miR-506-3p/ETS1/RAS/ERK after transfection was detected by qRT-PCR and Western blot using the same method above.

2.7. CCK-8

Cells were seeded in 96-well plates at 5000/well and incubated a condition containing 5 % CO_2 at 37 °C. At 24 h and 48 h after incubation, 10 μL of Cell Counting Kit-8 (CCK-8) (Sigma-Aldrich, USA) was added in to the plates. The absorbance was measured at 450 nm using a microplate reader.

2.8. Cell scratch assay

The concentration of cell suspension was adjusted to 5×10^6 cells/mL with trypsin, inoculated into 6-well plates, and 3 scratches were made in the 6-well plates with a sterilized tip when the cell fusion rate achieved about 75 %; the dropped cells were washed with PBS, and the plates were cultured for 24 h. An inverted fluorescence microscope was applied for photo taking, and the scratch width at different points were measured to calculate the average value of scratch fusion rate. Cell scratch rate = (initial scratch width - cell migration distance)/initial scratch width × 100 %

2.9. Transwell

A sterile Transwell chamber was placed in a 24-well plate. The liquid Matrigel matrix gel was diluted at 1:5 and added into the Transwell chamber at 50 μL/well, so that the gel was evenly leveled. After the gel was solidified, add 500 μL of culture medium into the 24-well plate, add 200 μL of cell suspension to the upper chamber, with about 20000 cells per well. After incubation for 24 h, the liquid in the upper chamber was discarded; the chamber was washed twice with PBS and allowed to dry in the air; cells penetrating the membrane in the upper chamber were soaked and fixed with 4 % paraformaldehyde (30 min), rinsed with PBS, and dipped in crystal violet staining solution for 5 min; the excess crystal violet on the surface was gently rinsed with PBS. Cells were observed under the microscope and photographed, and the number of cells was counted.

2.10. TUNEL staining

Cells were seeded on round slides, fixed with paraformaldehyde for 30 min, rinsed with PBS, incubated with cell permeabilization buffer for 2 min at room temperature, and marked in accordance with the instruction for use of the Terminal Deoxynucleotidyl Transferase Mediated dUTP Nick End Labeling (TUNEL) kit (Vazyme; USA); images were captured with a fluorescence microscope and analyzed with software Image J (National Institutes of Health, USA).

2.11. Effect of SNHG16 on KIRC cells via miR-506-3p/ETS1/RAS/ERK

KIRC cells in logarithmic phase were divided into 6 groups and transfected (intervened) as follows: Normal group: normal culture; Group A: co-transfection with over-expressed SNHG16 and ETS1 plasmids, miR-506-3p mimic sequence, and RAS/ERK pathway activator (RASAL1); Group B: co-transfection with over-expressed SNHG16 plasmid and RASAL1; Group C: co-transfection with over-

expressed SNHG16 plasmid and miR-506-3p mimic sequence; Group D: co-transfection with over-expressed SNHG16 and ETS1 plasmids. Group E: co-transfection with over-expressed ETS1 plasmid and miR-506-3p mimic sequence. In addition, the biological behaviors of transfected cells were determined based on the protocol above.

2.12. Effect of miR-506-3p/ETS1 on RAS/ERK signaling pathway

The miR-506-3p mimic, inhibitor sequence, negative control group, over-expressed ETS1 plasmid, silenced plasmid and blank control were separately transfected into KIRC cells to determine the expression of the RAS/ERK signaling pathway. The effect of miR-506-3p and ETS1 on the RAS/ERK signaling pathway was determined in the same way as mentioned above.

2.13. Animal information

Eighteen healthy BALB/c nude mice of SPF grade were purchased from Nanjing Amphibian Biomedical Technology Co. 6–8 weeks old, body mass 18–20 g. Adaptive feeding for 1 week at $(25 \pm 2)^{\circ}C$, humidity $(50 \pm 10)\%$, 12 h day/night alternation, free feeding and drinking.

2.14. Nude mice tumorigenesis assay

Mice were randomly divided into 3 groups ($n = 6$), and the cells of normal group, mimics group and si-SNHG16 group (ACHN) were resuspended with PBS, and 500 μL (1×10^7/mL) were aspirated and injected into the right axilla of mice subcutaneously, and then continued to be fed. Three mice from each of the three groups were randomly selected and executed at 7 d and 14 d, respectively, and the intact tumor tissues were removed to observe the growth of tumors and measure the volume and mass.

2.15. Statistical analysis

SPSS22.0 (IBM, USA) and GraphPad Prism6 (GraphPad Software) were separately used for statistical analysis and plotting. All the results were expressed as $(\bar{\chi} \pm s)$. T-test was adopted for intra-group comparison, and Analysis of Variance and Bonferroni test for inter-group comparison, diagnostic value using receiver operating characteristic (ROC) curve analysis. $P < 0.05$ was considered as statistically significant.

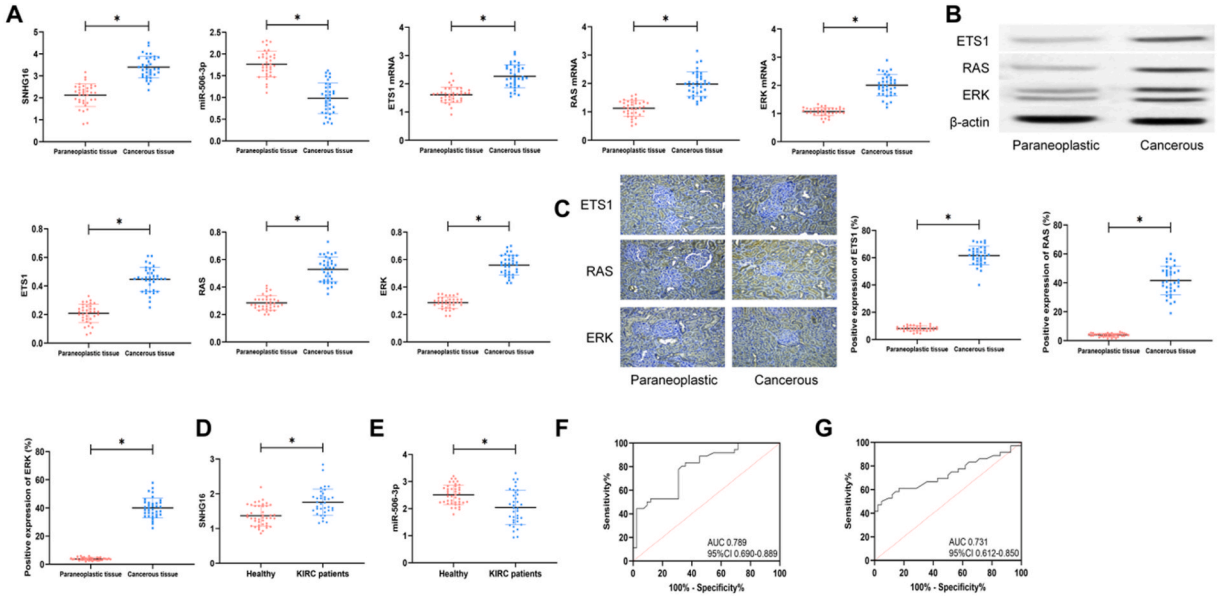

Fig. 1. Expression of SNHG16/miR-506-3p/ETS1/RAS/ERK in tissues. A, Comparison of SNHG16/miR-506-3p/ETS1/RAS/ERK expression in cancer and paraneoplastic tissues. B, Western blot detection of ETS1/RAS/ERK expression in cancer and paraneoplastic tissues. C, Immunohistochemical detection of positive expression of ETS1/RAS/ERK in cancer and paraneoplastic tissues. A, Comparison of the expression levels of SNHG16 in serum. B, Comparison of the expression levels of miR-506-3p in serum. C, ROC curve of SNHG16 diagnostic KIRC. D, ROC curve of miR-506-3p diagnostic KIRC. *$P < 0.05$. Fig. 1B uncut original image in Supplementary Fig. S1.

3. Results

3.1. Expression of SNHG16/miR-506-3p/ETS1/RAS/ERK in tissues

Compared with adjacent tissues, the expression of SNHG16, ETS1 mRNA, RAS mRNA and ERK mRNA in carcinoma tissues were significantly higher, while miR-506- 3p was significantly lower ($P < 0.05$, Fig. 1A). The expression of ETS1/RAS/ERK protein also revealed that the expression of ETS1, RAS and ERK increased in carcinoma tissues ($P < 0.05$, Fig. 1B). According to the results of immunohistochemical, significantly high expression of ETS1, RAS and ERK was observed in carcinoma tissues of patients with KIRC. (Fig. 1C). Detection of the expression levels of SNHG16 and miR-506-3p in the serum of KIRC patients and physical examiners showed that SNHG16 was significantly higher in KIRC patients than in physical examiners, while miR-506-3p was lower than in physical examiners ($P < 0.05$, Fig. 1D/E). By ROC analysis, it was seen that when SNHG16 > 1.41 in serum, the sensitivity of diagnosing the occurrence of KIRC was 83.33 % and the specificity was 64.29 % ($P < 0.05$, Fig. 1F). And when miR-506-3p < 2.02, the sensitivity and specificity of diagnosing KIRC were 50.00 % and 95.24 %, respectively ($P < 0.05$). (Fig. 1G).

3.2. Expression of SNHG16/miR-506-3p/ETS1/RAS/ERK in cells

After transfection, the expression of SNHG16 in the mimics group was higher than that in the blank group and the si-SNHG16 group, and the expression of SNHG16 in the si-SNHG16 group was lower than that in the blank group ($P < 0.05$, Fig. 2A/B), indicating successful transfection. Subsequently, miR-506-3p/ETS1/RAS/ERK expression was determined. The expression of miR-506-3p was the lowest in the mimics group and the highest in the si-SNHG16 group ($P < 0.05$). The expression of ETS1, RAS and ERK increased in the mimics group but decreased in the si-SNHG16 group ($P < 0.05$). (Fig. 2C/D).

3.3. Effects of SNHG16 on cell biological behavior

After transfection, the proliferation, invasion and migration of KIRC cells in the mimics group were higher than those in the control group. In contrast, the proliferation, invasion and migration rates of the si-SNHG16 group were lower than those of the control group ($P < 0.05$). (Fig. 3A–E). TUNEL staining showed that the number of apoptotic cells in the si-SNHG16 group was high among the three groups, and the number of apoptotic cells in the mimics group was lower than that in the si-SNHG16 group and higher than that in the blank group ($P < 0.05$). (Fig. 3F).

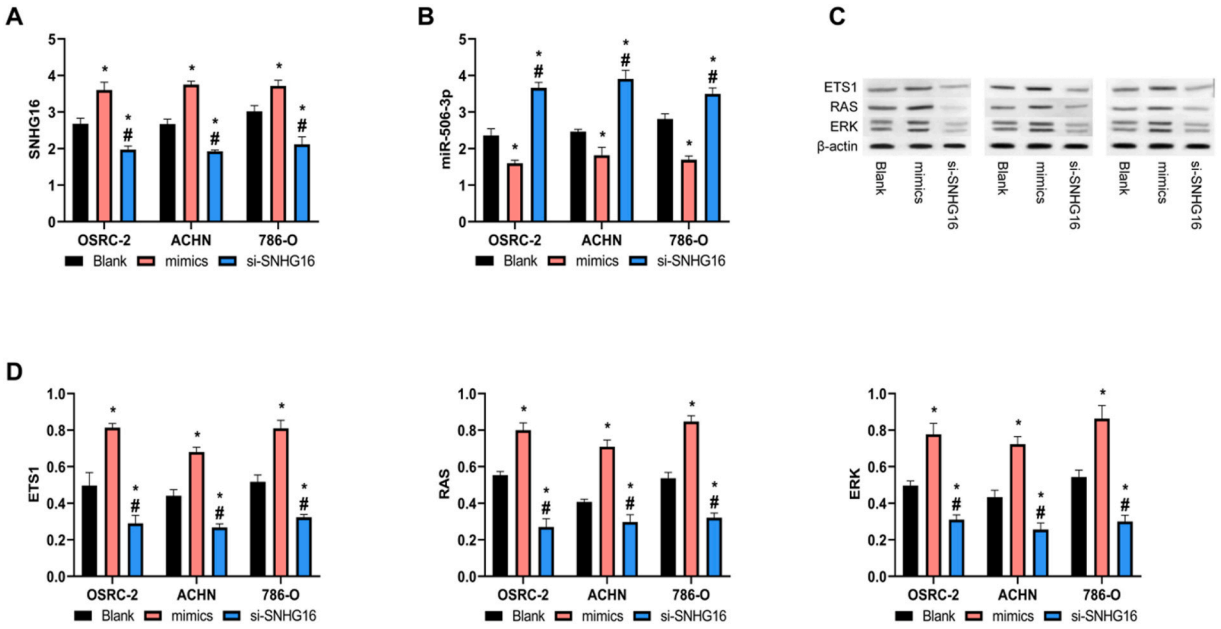

Fig. 2. Expression of SNHG16/miR-506-3p/ETS1/RAS/ERK in cells. A, Comparison of the expression levels of SNHG16 in cells after transfection with SNHG16 aberrant expression vector. B, Effect of SNHG16 on miR-506-3p expression levels. C and D, Western blot detection of ETS1/RAS/ERK expression levels in cells after transfection with SNHG16 aberrant expression vector and quantitative analysis results. * indicates a statistically significant difference from the Blank group and # indicates a statistically significant difference from the mimics group ($P < 0.05$). Fig. 2C uncut original image in Supplementary Fig. S2.

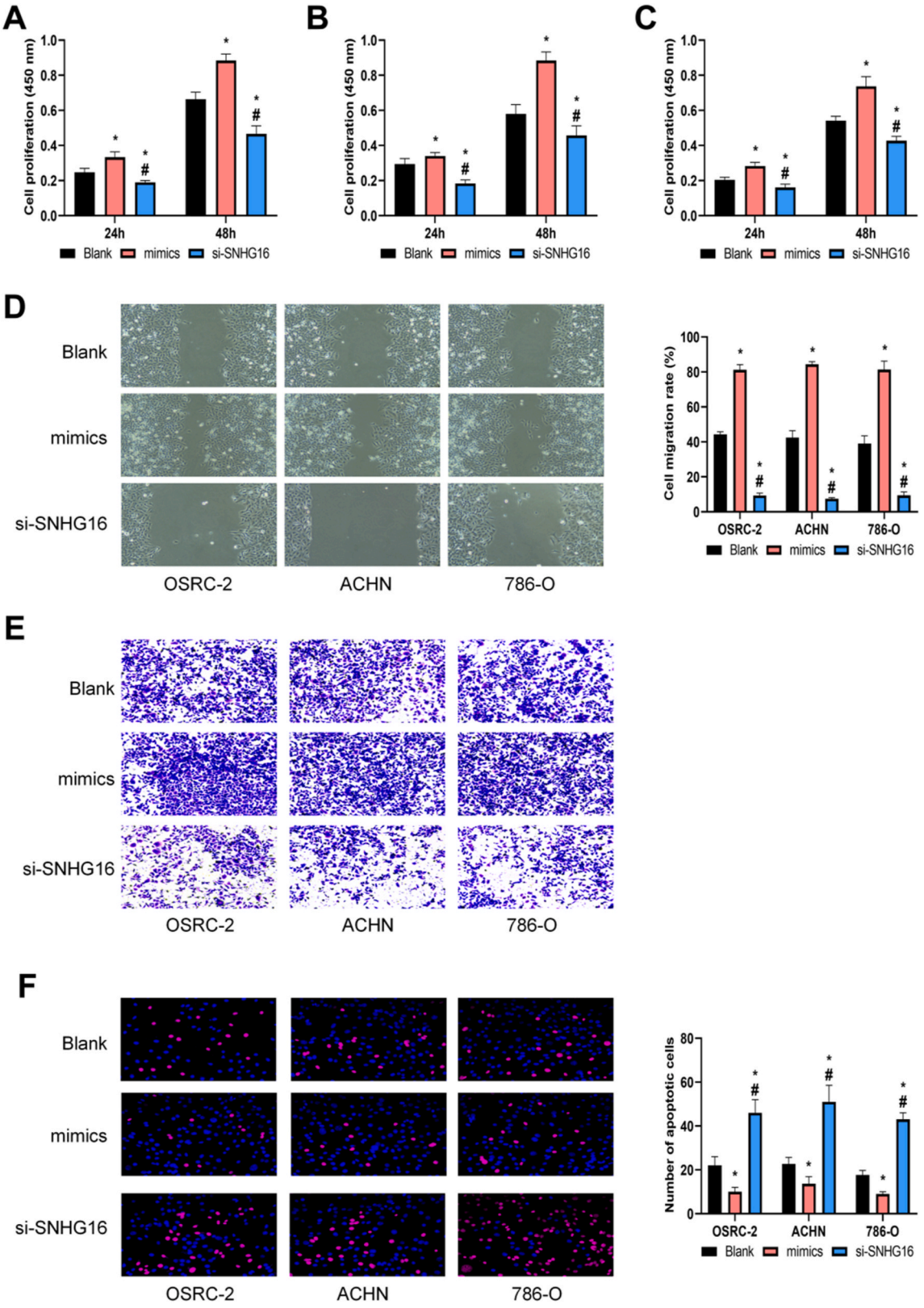

(caption on next page)

Fig. 3. Effect of SNHG16 on cellular activity. A, Results of the CCK-8 experiment for OSRC-2. B, Results of the CCK-8 experiment for ACHN. C, Results of the CCK-8 experiment for 786-O. D, Results of cell scratching experiments. E, Transwell experimental results. F, Effect of SNHG16 on apoptosis, red fluorescence indicates apoptotic cells. * indicates a statistically significant difference from the Blank group and # indicates a statistically significant difference from the mimics group ($P < 0.05$). (For interpretation of the references to color in this figure legend, the reader is referred to the Web version of this article.)

3.4. Effects of SNHG16 on biological behavior of KIRC cells via miR-506-3p/ETS1/RAS/ERK cellular activity

After transfection with abnormally expressed miR-506-3p/ETS1 sequence/plasmid and RAS/ERK activator, the normal group, Group C, and Group E showed consistent biological behavior, and Group B and Group D showed consistent biological behavior ($P > 0.05$). The invasion and migration rate of Group A were the highest among the six groups ($P < 0.05$), followed by Groups B and D, and then the normal group and Groups C and E ($P < 0.05$). (Fig. 4A–D). Similarly, there was no significant difference in apoptosis among the normal group, Group C and Group E, and no difference between Group B and Group D ($P > 0.05$). Apoptotic cells in group A were the lowest among the 6 groups. The number of apoptotic cells of Group A was the lowest among the six groups, followed by Groups B and D, and then the normal group and Groups C and E ($P < 0.05$). (Fig. 4E–G).

3.5. Effect of miR-506-3p/ETS1 on RAS/ERK signaling pathway

The expression of RAS and ERK were obviously decreased in cells after transfection with miR-506-3p-mimics compared with the blank group, while the expression of RAS and ERK were significantly increased in cells after transfection with miR-506-3p-inhibitors ($P < 0.05$). The expression of RAS and ERK increased after transfection with over-expressed ETS1 plasmid, but decreased after transfection with silenced ETS1 expression sequence ($P < 0.05$). (Fig. 5A/B).

3.6. Effect of SNHG16 on in vivo tumors

Finally, in the tumorigenesis experiment in nude mice, it was seen that there was no significant difference in tumor weight and volume between the normal and mimics groups at 7 d ($P < 0.05$), while the weight and volume in the si-SNHG16 group were slightly lower ($P < 0.05$). At 14 d, the tumor weight and volume in the mimics group were the highest among the three groups, while the tumor weight and volume in the si-SNHG16 group were lower than those in the blank group ($P < 0.05$). The subcutaneous tumor growth in all three groups increased significantly at 14 d compared with that at 7 d ($P < 0.05$). (Fig. 6A–C).

4. Discussion

KIRC is the subtype with the highest malignancy and the worst prognosis in RCC, so a deep understanding of its pathogenic mechanism is clinically significant for the future diagnosis and treatment of KIRC [23]. In previous studies, SNHG16 has been preliminarily confirmed to regulate the progression of KIRC [14]; for its clinical application, however, more studies are needed to verify its mechanism of action. Therefore, the study was conducted to analyze the role of SNHG16 in KIRC as follows. Through our experiments, we found that SNHG16 and ETS1 were highly expressed and miR-506-3p was lowly expressed in KIRC tissues, and the RAS/ERK signaling pathway was significantly activated. Furthermore, SNHG16 regulates the biological behavior of KIRC cells by targeting the miR-506-3p/ETS1/RAS/ERK molecular axis. These results provide new research directions for future diagnosis and treatment of KIRC.

First, SNHG16 expression is obviously higher in KIRC patients, similar to the findings of Xiang Z et al. and Chen L et al. [24,25]. In the cellular assay, the proliferation, invasion and migration capabilities of KIRC cells were significantly enhanced and the apoptosis rate was decreased after SNHG16 expression elevation. This once again confirmed that the highly expressed SNHG16 acts as an oncogene in KIRC, and SNHG16 silence can inhibit the malignant progression of KIRC, indicating that SNHG16 is a potential targeted therapeutic approach for KIRC in the future. Previous studies have suggested that inhibition of SNHG16 slows down the progression of malignant tumors [26,27], so the above results are also expected.

In molecular pathogenesis studies of tumors, lncRNAs usually exert its biological regulatory effects through multiple pathways [28]. Although previous studies and the above experiments have fully verified the role of SNHG16 in KIRC, its mechanism of action should be analyzed. In the preliminary preparation of the experiment, a ceRNA network was constructed with SNHG16, and the miRNAs and downstream target genes related to SNHG1 were predicted by bioinformatics methods. Among these SNHG1-related miRNAs and target genes, the binding site of SNHG16 to miR-506-3p was identified. In addition, studies have also shown that miR-506-3p is up-regulated in vascular smooth muscle, affecting the proliferation, migration, differentiation and contraction of vascular smooth muscle cells [29]. Therefore, it was hypothesized that SNHG16 may be involved in the alteration of biological behavior of KIRC cells through miR-506-3p. In order to verify this conjecture, the expression of the above molecular pathways in KIRC tissues was also observed. Decreased miR-506-3p and increased ETS-1 were witnessed, as well as obviously activated Ras/ERK signaling pathway, which preliminarily confirmed that they may be involved in the occurrence and development of KIRC. What mentioned above are also consistent with the results of relevant studies [30–32], proving the accuracy of the results. Not only that, considering that peripheral blood is more convenient to collect and has higher clinical applicability, we performed ROC analysis for the expression of SNHG16 and miR-506-3p in peripheral blood. And the results showed that both showed excellent results for the diagnosis of KIRC. This suggests that in the future, SNHG16 and miR-506-3p also have the potential to become objective assessment indicators of

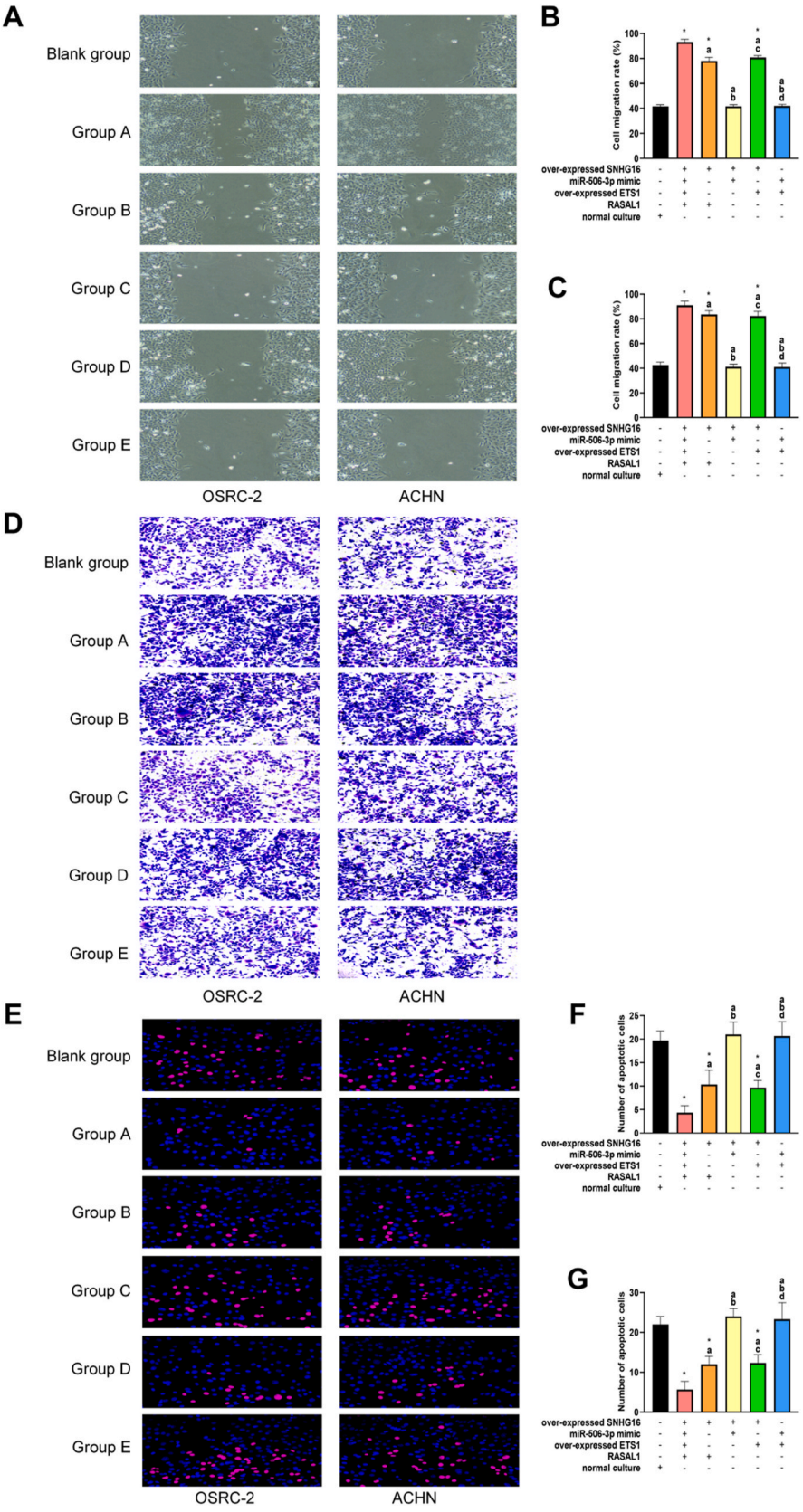

(caption on next page)

Fig. 4. Effect of SNHG16 on cellular activity via miR-506-3p/ETS1/RAS/ERK. A, Results of cell scratching experiments. B, Migration rate of OSRC-2. C, Migration rate of ACHN. D, Transwell experimental results. E, Results of TUNEL staining experiments. F, Apoptotic cells in OSRC-2 (red fluorescence). G, Apoptotic cells in ACHN (red fluorescence). *, a,b,c,d indicate statistically significant differences with blank group, group A, group B, group C, and group D, respectively ($P < 0.05$). (For interpretation of the references to color in this figure legend, the reader is referred to the Web version of this article.)

KIRC, thus aiding in better diagnosis of the occurrence and development of KIRC.

Elevated SNHG1 was observed after transfection with abnormally expressed SNHG1, as well as increased ETS-1 and Ras/ERK signaling pathway and decreased miR-506-3p in KIRC cells, and silencing SNHG1 achieved opposite results, suggesting that the molecular pathway above was also involved in the process of SNHG1 affecting the biological behavior of KIRC cells. In previous studies, although the regulation of miR-506-3p/ETS1/RAS/ERK activity in tumor cells such as gastric and esophageal carcinomas has been shown [33–35], their role in KIRC remains to be verified. More experiments are still needed to confirm the pathway of action of SNHG1 in relation to miR-506-3p/ETS1/RAS/ERK. The rescue experiment revealed that there was no significant difference in the biological behavior of cells between Groups C and E and the normal group, suggesting that the effects of elevated SNHG16 on KIRC cells were reversed by simultaneous increase in miR-506-3p, and the effects of miR-506-3p could be reversed by ETS1. Consistent biological behavior indicated that activation of the RAS/ERK pathway had the same effect as increase in ETS1, which further worsened the malignancy of KIRC. Both elevated miR-506-3p and silenced ETS1 inhibited the status of RAS/ERK. Thus, there is a clear inter-regulatory relationship of the molecular axis in regulating the biological behavior of KIRC cells, which also verified our point of view. Finally, in tumorigenic experiments in nude mice, we saw a significant inhibition of in vivo tumor growth following silencing of SNHG16 expression, which confirmed the effect of SNHG16 on KIRC and could lay a solid foundation for its subsequent clinical application. Based on the results obtained from the above experiments, it was believed that SNHG16 regulates the biological behavior of KIRC by targeting miR-506- 3p and ETS1 to activate the RAS/ERK signaling pathway, which provides a reliable reference for future molecular immunotherapy targeting SNHG16.

However, the experimental conditions are limited, so more experiments are needed to validate the targeting relationship between SNHG16/miR-506-3p/ETS1; the changes in the above molecular axis may be observed through reverse regulation of RAS/ERK signaling pathway to understand the specific mechanism of this pathway more clearly. In addition, in vivo animal experiments should be conducted to demonstrate the effect of SNHG16 silence on actual tumorigenesis, so as to lay a more reliable foundation for future clinical diagnosis and treatment of SNHG16.

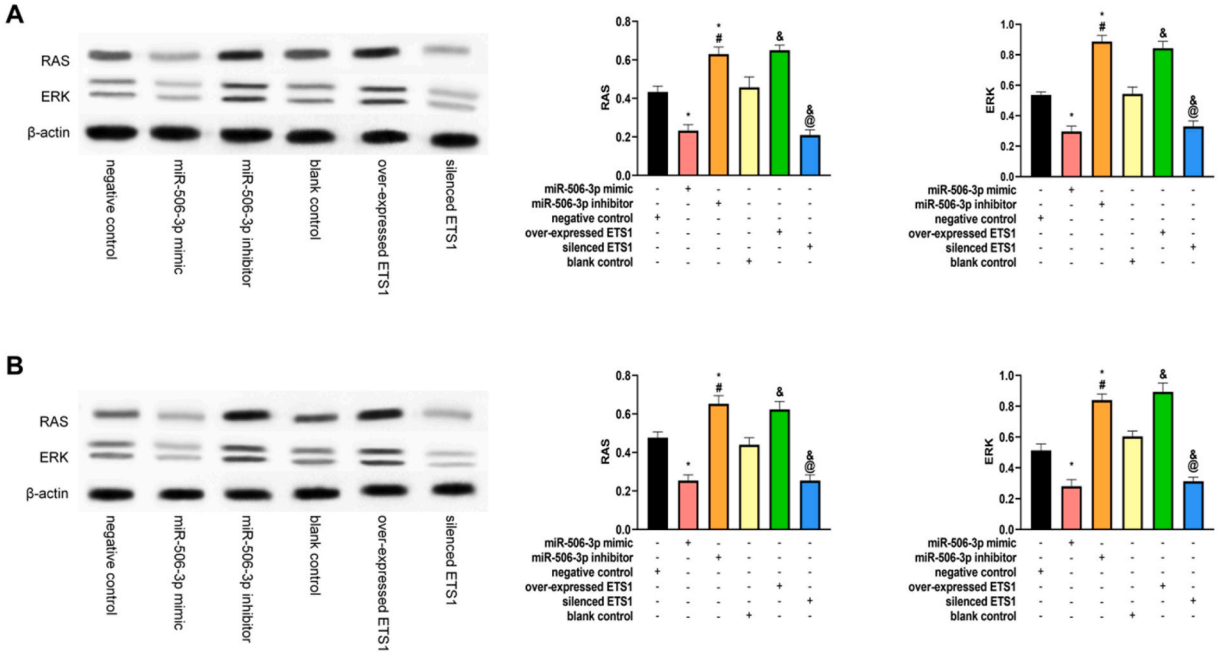

Fig. 5. Effect of miR-506-3p/ETS1 on RAS/ERK signaling pathway. A, Effect of miR-506-3p/ETS1 on the RAS/ERK signaling pathway in OSRC-2. B, Effect of miR-506-3p/ETS1 on the RAS/ERK signaling pathway in ACHN. *, #, & and @ indicate statistically significant differences between and negative control sequences, miR-506-3p mimics sequences, blank control and overexpression of ETS1 plasmids, respectively ($P < 0.05$). Fig. 5A and B uncut original image in Supplementary Figs. S3 and S4.

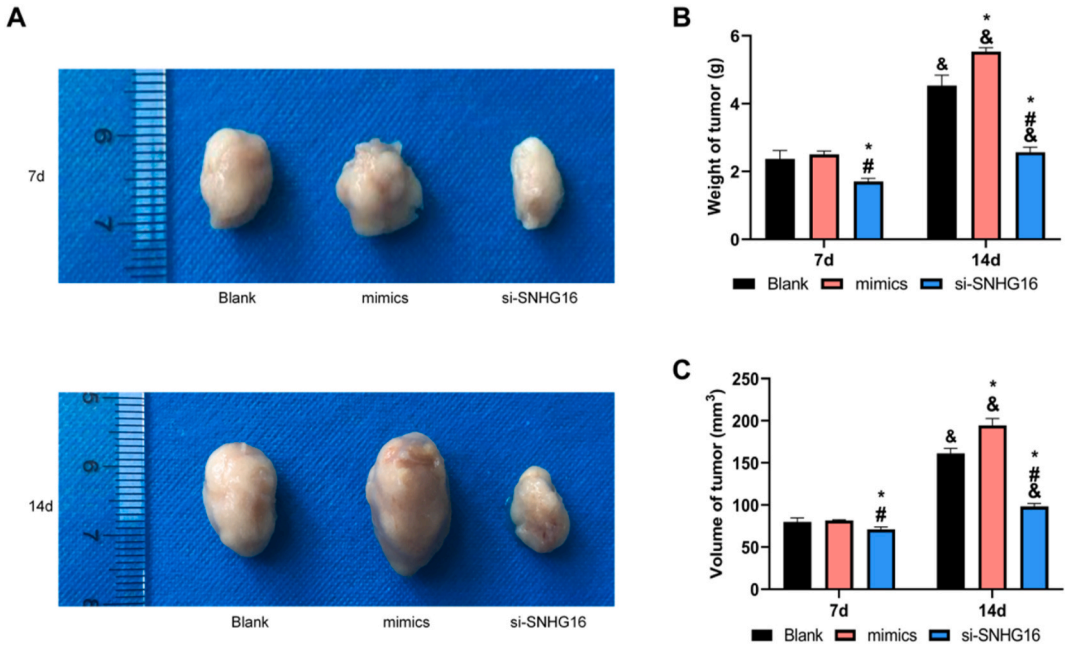

Fig. 6. Effect of SNHG16 on in vivo tumors. A, Complete photo of the tumor. B, Comparison of the weight of the tumors. C, Comparison of the volume of the tumor. * indicates a statistically significant difference from the Blank group, # indicates a statistically significant difference from the mimics group and & indicates a statistically significant difference from that at 7 d ($P < 0.05$).

5. Conclusion

SNHG16 was highly expressed in KIRC and promoted the malignant growth of tumor cells by regulating miR-506-3p/ETS1 to activate the RAS/ERK signaling pathway, which provides theoretical basis for the design and development of new drugs and the establishment of new gene therapies that intervene in signal transduction-related boot genes in the early stages, to improve the prognosis and safety of KIRC patients.

Ethical approval

The study protocol was approved by the Ethics Committee of The Second Affiliated Hospital of Bengbu Medical College (Approval No.2023-279); The animal experimental protocols were approved by the Animal Ethics Committee of The Second Affiliated Hospital of Bengbu Medical College (Approval No.2023-632).

Availability of data and materials

The datasets used and/or analyzed during the current study are available from the corresponding author on reasonable request.

Fund

This research was funded by Natural Science Key Project of Anhui Provincial Education Department (NO.2022AH051516).

CRediT authorship contribution statement

Tao Cheng: Writing – original draft. **Ming-Li Gu:** Funding acquisition, Conceptualization. **Wei-Qiang Xu:** Writing – review & editing. **Da-Wen Ye:** Visualization. **Ze-Yu Zha:** Validation. **Wen-Ge Fang:** Supervision. **Li-Kai Mao:** Software. **Jing Ning:** Methodology. **Xing-Bang Hu:** Data curation. **Yong-Hui Ding:** Formal analysis.

Declaration of competing interest

The authors declare the following financial interests/personal relationships which may be considered as potential competing interests:Mingli Gu reports financial support was provided by Natural Science Key Project of Anhui Provincial Education Department. If there are other authors, they declare that they have no known competing financial interests or personal relationships that could have appeared to influence the work reported in this paper.

Acknowledgements

Thanks to the Anhui Higher Education Scientific Research Project for supporting this work.

Appendix A. Supplementary data

Supplementary data to this article can be found online at https://doi.org/10.1016/j.heliyon.2024.e30388.

References

[1] S. Bahadoram, M. Davoodi, S. Hassanzadeh, M. Bahadoram, M. Barahman, L. Mafakher, Renal cell carcinoma: an overview of the epidemiology, diagnosis, and treatment, G. Ital. Nefrol. 39 (3) (2022).
[2] J. Lobo, R. Ohashi, M.B. Amin, D.M. Berney, E.M. Comperat, I.A. Cree, A.J. Gill, A. Hartmann, S. Menon, G.J. Netto, M.R. Raspollini, M.A. Rubin, P.H. Tan, S. K. Tickoo, T. Tsuzuki, S. Turajlic, M. Zhou, J.R. Srigley, H. Moch, WHO 2022 landscape of papillary and chromophobe renal cell carcinoma, Histopathology 81 (4) (2022) 426–438.
[3] Z. Li, H. Xu, L. Yu, J. Wang, Q. Meng, H. Mei, Z. Cai, W. Chen, W. Huang, Patient-derived renal cell carcinoma organoids for personalized cancer therapy, Clin. Transl. Med. 12 (7) (2022) e970.
[4] S. Angori, J. Lobo, H. Moch, Papillary renal cell carcinoma: current and controversial issues, Curr. Opin. Urol. 32 (4) (2022) 344–351.
[5] A. Siddiqi, M. Rani, P. Bansal, M.M.A. Rizvi, Renal cell carcinoma management: a step to nano-chemoprevention, Life Sci. 308 (2022) 120922.
[6] E. Jonasch, C.L. Walker, W.K. Rathmell, Clear cell renal cell carcinoma ontogeny and mechanisms of lethality, Nat. Rev. Nephrol. 17 (4) (2021) 245–261.
[7] M.C. Bridges, A.C. Daulagala, A. Kourtidis, LNCcation: lncRNA localization and function, J. Cell Biol. 220 (2) (2021).
[8] T. Nojima, N.J. Proudfoot, Mechanisms of lncRNA biogenesis as revealed by nascent transcriptomics, Nat. Rev. Mol. Cell Biol. 23 (6) (2022) 389–406.
[9] E.K. Robinson, S. Covarrubias, S. Carpenter, The how and why of lncRNA function: an innate immune perspective, Biochim Biophys Acta Gene Regul. Mech. 1863 (4) (2020) 194419.
[10] Z. Yang, Q. Li, X. Zheng, L. Xie, Long noncoding RNA small nucleolar host gene: a potential therapeutic target in urological cancers, Front. Oncol. 11 (2021) 638721.
[11] A. Biagioni, S. Tavakol, N. Ahmadirad, M. Zahmatkeshan, L. Magnelli, A. Mandegary, H. Samareh Fekri, M.H. Asadi, R. Mohammadinejad, K.S. Ahn, Small nucleolar RNA host genes promoting epithelial-mesenchymal transition lead cancer progression and metastasis, IUBMB Life 73 (6) (2021) 825–842.
[12] L. Huang, X. Jiang, Z. Wang, X. Zhong, S. Tai, Y. Cui, Small nucleolar RNA host gene 1: a new biomarker and therapeutic target for cancers, Pathol. Res. Pract. 214 (9) (2018) 1247–1252.
[13] C.Y. Gong, R. Tang, W. Nan, K.S. Zhou, H.H. Zhang, Role of SNHG16 in human cancer, Clin. Chim. Acta 503 (2020) 175–180.
[14] T. Cheng, W. Shuang, D. Ye, W. Zhang, Z. Yang, W. Fang, H. Xu, M. Gu, W. Xu, C. Guan, SNHG16 promotes cell proliferation and inhibits cell apoptosis via regulation of the miR-1303-p/STARD9 axis in clear cell renal cell carcinoma, Cell. Signal. 84 (2021) 110013.
[15] J. Wang, S. Zhao, J. Sun, X. Wang, M. Guan, J. Yin, B. Tang, Oncogenic role and potential regulatory mechanism of fatty acid binding protein 5 based on a pan-cancer analysis, Sci. Rep. 13 (1) (2023) 4060.
[16] Y.J. Guo, W.W. Pan, S.B. Liu, Z.F. Shen, Y. Xu, L.L. Hu, ERK/MAPK signalling pathway and tumorigenesis, Exp. Ther. Med. 19 (3) (2020) 1997–2007.
[17] J.Y. Fang, B.C. Richardson, The MAPK signalling pathways and colorectal cancer, Lancet Oncol. 6 (5) (2005) 322–327.
[18] E. Santos, P. Crespo, The RAS-ERK pathway: a route for couples, Sci. Signal. 11 (554) (2018).
[19] M.A. Zaballos, A. Acuna-Ruiz, M. Morante, P. Crespo, P. Santisteban, Regulators of the RAS-ERK pathway as therapeutic targets in thyroid cancer, Endocr. Relat. Cancer 26 (6) (2019) R319–R344.
[20] F. Calvo, L. Agudo-Ibanez, P. Crespo, The Ras-ERK pathway: understanding site-specific signaling provides hope of new anti-tumor therapies, Bioessays 32 (5) (2010) 412–421.
[21] J.P. Plotnik, J.A. Budka, M.W. Ferris, P.C. Hollenhorst, ETS1 is a genome-wide effector of RAS/ERK signaling in epithelial cells, Nucleic Acids Res. 42 (19) (2014) 11928–11940.
[22] K. Abe, H. Nakashima, M. Ishida, N. Miho, M. Sawano, N.N. Soe, M. Kurabayashi, K. Chayama, M. Yoshizumi, T. Ishida, Angiotensin II-induced osteopontin expression in vascular smooth muscle cells involves Gq/11, Ras, ERK, Src and Ets-1, Hypertens. Res. 31 (5) (2008) 987–998.
[23] H. Xu, X. Zheng, S. Zhang, X. Yi, T. Zhang, Q. Wei, H. Li, J. Ai, Tumor antigens and immune subtypes guided mRNA vaccine development for kidney renal clear cell carcinoma, Mol. Cancer 20 (1) (2021) 159.
[24] Z. Xiang, G. Huang, H. Wu, Q. He, C. Yang, R. Dou, Q. Liu, J. Song, Y. Fang, S. Wang, B. Xiong, SNHG16 upregulation-induced positive feedback loop with YAP1/TEAD1 complex in Colorectal Cancer cell lines facilitates liver metastasis of colorectal cancer by modulating CTCs epithelial-mesenchymal transition, Int. J. Biol. Sci. 18 (14) (2022) 5291–5308.
[25] L. Chen, C.H. Qiu, Y. Chen, Y. Wang, J.J. Zhao, M. Zhang, LncRNA SNHG16 drives proliferation, migration, and invasion of lung cancer cell through modulation of miR-520/VEGF axis, Eur. Rev. Med. Pharmacol. Sci. 24 (18) (2020) 9522–9531.
[26] F. Xu, G. Zha, Y. Wu, W. Cai, J. Ao, Overexpressing lncRNA SNHG16 inhibited HCC proliferation and chemoresistance by functionally sponging hsa-miR-93, OncoTargets Ther. 11 (2018) 8855–8863.
[27] J.M. Westendorf, A. Schonbrunn, Peptide specificity for stimulation of corticotropin secretion: activation of overlapping pathways by the vasoactive intestinal peptide family and corticotropin-releasing factor, Endocrinology 116 (6) (1985) 2528–2535.
[28] Y.T. Tan, J.F. Lin, T. Li, J.J. Li, R.H. Xu, H.Q. Ju, LncRNA-mediated posttranslational modifications and reprogramming of energy metabolism in cancer, Cancer Commun. 41 (2) (2021) 109–120.
[29] H. Dong, G. Jiang, J. Zhang, Y. Kang, MiR-506-3p promotes the proliferation and migration of vascular smooth muscle cells via targeting KLF4, Pathobiology 88 (4) (2021) 277–288.
[30] N.H. Chou, Y.H. Lo, K.C. Wang, C.H. Kang, C.Y. Tsai, K.W. Tsai, MiR-193a-5p and -3p play a distinct role in gastric cancer: miR-193a-3p suppresses gastric cancer cell growth by targeting ETS1 and CCND1, Anticancer Res. 38 (6) (2018) 3309–3318.
[31] W.J. Jeong, E.J. Ro, K.Y. Choi, Interaction between Wnt/beta-catenin and RAS-ERK pathways and an anti-cancer strategy via degradations of beta-catenin and RAS by targeting the Wnt/beta-catenin pathway, npj Precis. Oncol. 2 (1) (2018) 5.
[32] Y.H. Pan, J. Chen, C. Sun, J.F. Ma, X. Li, Effect of Ras-guanine nucleotide release factor 1-mediated H-Ras/ERK signaling pathway on glioma, Brain Res. 1754 (2021) 147247.
[33] Y. Ding, S. Gao, J. Zheng, X. Chen, Blocking lncRNA-SNHG16 sensitizes gastric cancer cells to 5-Fu through targeting the miR-506-3p-PTBP1-mediated glucose metabolism, Cancer Metab. 10 (1) (2022) 20.
[34] L. Ding, L. Wang, Z. Li, X. Jiang, Y. Xu, N. Han, The positive feedback loop of RHPN1-AS1/miR-1299/ETS1 accelerates the deterioration of gastric cancer, Biomed. Pharmacother. 124 (2020) 109848.
[35] M. Li, X. Li, S. Chen, T. Zhang, L. Song, J. Pei, G. Sun, L. Guo, IPO5 mediates EMT and promotes esophageal cancer development through the RAS-ERK pathway, Oxid. Med. Cell. Longev. 2022 (2022) 6570879.